SIAM J. APPL. MATH.
Vol. 70, No. 4, pp. 1305–1329

MODELLING OF AND MIXED FINITE ELEMENT METHODS FOR GELS IN BIOMEDICAL APPLICATIONS*

MARIE E. ROGNES†, M.-CARME CALDERER‡, AND CATHERINE A. MICEK‡

Abstract. A set of equilibrium equations for a biphasic polymer gel are considered with the end purpose of studying stress and deformation in confinement problems encountered in connection with biomedical implants. The existence of minimizers for the gel energy is established first. Further, the small-strain equations are derived and related to the linear elasticity equations with parameters dependent on the elasticity of the polymer and the mixing of the polymer and solvent. Two numerical methods are considered, namely a two-field displacement-pressure formulation and a three-field stress-displacement-rotation formulation with weakly imposed symmetry. The symmetry of the stress tensor is affected by the residual stress induced by the polymer-solvent mixing. A novel variation of the stress-displacement formulation of linear elasticity with weak symmetry is therefore proposed and analyzed. Finally, the numerical methods are used to simulate the stresses arising in a confined gel implant.

Key words. gels, mixed finite element, residual stress, hyperelasticity, polyconvexity

AMS subject classifications. 74S05, 65Z05

DOI. 10.1137/090754443

1. Introduction.

Since the development and commercialization of the pacemaker in 1957, a wide variety of biomedical devices have been designed to address chronic health conditions. In addition to the pacemaker, other examples of *body implantable devices* include artificial bone tissue and cardiovascular stents. When designing such devices, their long-term use must be taken into account. Many of these devices are made of synthetic polymers, and, upon insertion in the human body, the absorption of moisture can cause the polymer to swell. The combination of swelling and confinement causes stresses that may compromise the intended lifetime of the device. For example, in devices such as artificial bones that are attached with a chemical glue, the stress buildup along the attachment can loosen the glue and destroy device performance. Hence, the impact of the body environment on a device is an important aspect of body implantable devices. In particular, the ability to predict the resulting stresses may be crucial to effective design.

Polymers that have absorbed moisture classify as gels, and many biomedical devices use polymers in a gel form. The term *gel* refers to cross-linked polymer networks or entanglements enclosing a solvent such as water. The two components of the gel coexist by balancing each other. The polymer network confines the liquid solvent, and the solvent ensures that the polymer does not collapse into a dry state. Thus, gels typically have the appearance of solids and may in many situations behave as such.

*Received by the editors March 30, 2009; accepted for publication (in revised form) July 28, 2009; published electronically October 22, 2009.
http://www.siam.org/journals/siap/70-4/75444.html

†Center for Biomedical Computing, Simula Research Laboratory, P.O. Box 134, 1325 Lysaker, Norway (meg@simula.no). The work of this author is supported by a Center of Excellence grant from the Norwegian Research Council to the Centre of Mathematics for Applications at the University of Oslo. This work is also supported by a Center of Excellence grant from the Norwegian Research Council to the Center for Biomedical Computing at Simula Research Laboratory.

‡School of Mathematics, University of Minnesota, 127 Vincent Hall, 206 Church Street S.E., Minneapolis, MN 55455 (mcc@math.umn.edu, mice0012@math.umn.edu). The work of these authors is partially supported by a grant from Medtronic, Inc., Twin Cities.

However, the pioneering work of Tanaka in the 1970s revealed some surprising physical properties [27]. One such property is the ability of the gel to display phase transitions. A gel phase transition is a finite change in volume of the polymer network—either a large expansion or contraction—that is induced by an infinitesimal change in the external environment. This and other properties of gels give an immensely rich array of applications [23, Vol. 3].

Due to their complex physical properties, the mathematical modelling of gels is a nontrivial task. Tanaka identified the following three forces acting on the polymer network and labeled their sum the osmotic pressure: the elasticity of the polymer network, the interaction of the polymer and solvent (also called the polymer-polymer affinity), and the ionization of the polymer network [27]. For the dynamics of gels, additional mechanisms, such as the diffusion of solvent and ions, the dynamics of the polymer network, and the dissipation of energy, must be accounted for. The modeling of gel dynamics has been an active field since the 1970s. Recent approaches in gel modelling include [8, 10, 18]. Also, the mechanics and modelling of biphasic soft tissue share common features with that of polymer gels. Mathematical models for gels may comprise fields such as deformation of the polymer network, velocities of polymer and solvent, pressures, stresses, and electrical and chemical concentrations. Clearly, the dynamical equations become a complicated system. Numerical methods are therefore essential for the solution and simulation of these equations.

The wide range of different modelling approaches makes direct comparison of simulation approaches challenging, but it is possible to identify some general trends. The flexibility of finite element methods with regard to complicated domain geometries has made them a natural choice for numerical simulations. In particular, mixed finite element methods approximating the velocities and pressure, possibly in combination with other variables, such as in [25], have been widespread. However, numerical stability considerations with respect to the material parameters and the mixed finite element spaces are rare in the literature. Some exceptions include the comparison of stabilized and stable velocity-pressure formulations for the deformation of biphasic soft tissue by Almeida and Spilker [1] and the study of an extended finite element method for the transitional interface dynamics of hydrogels by Dolbow, Fried, and Ji [11]. In this paper, the stability of the numerical methods with reference to the material parameters is carefully considered.

For biomedical devices such as artificial bone implants, the main question is the equilibrium state of the gel and the stress distribution in the gel and at interfaces. Accordingly, in this paper, we focus on the static equilibrium problem of nonionic gels. The starting point is taken from the equilibrium equations of [8], based on balance laws and the theory of mixtures, which again can be related to the series of papers of Yamaue and Doi [29, 30, 31] and the classical work of Flory [15]. The polymer network and polymer-solvent interaction contributions to the osmotic pressure are accounted for by the combination of an elastic and a mixing energy. Similar equations were treated by a deformation-based finite element method by Hong, Liu, and Sou [17]. Further, for this type of applications, the deformations are typically small, and thus the linearized regime may be relevant. Consequently, we shall derive the small-strain gel equilibrium equations. These reduce to the equations of linear elasticity, with Lamé coefficients additionally depending on the volume fraction of the polymer and the mixing energy. As the theory of finite element and mixed finite element methods for linear elasticity is very well-studied, we refer to [12] for a recent survey. Since the stress is of primary interest, we consider two numerical approaches, both offering higher order stress approximations, though in different ways. Both a two-field displacement-

pressure and a three-field stress-displacement-rotation mixed finite element method are presented and subsequently invoked.

To our knowledge, there are very few, if any, other works having studied mixed finite element methods of the stress-displacement-rotation type in the biphasic gel setting. The presence of the mixing energy gives additional features when compared to the purely elastic case. In particular, the state in which the residual stress vanishes is less intrinsic. The effect of nonvanishing residual stress due to nonequilibrium fractions of polymer is of direct physical interest and a key aspect of this work. Both the displacement-pressure and stress-displacement-rotation methods that we present allow for the possibility of nonvanishing residual stress. However, if the residual stress does not vanish, the linearized first Piola–Kirchhoff stress tensor is not symmetric, and thus the standard symmetry constraint of the stress tensor does not apply. Therefore, we propose a strategy for extending the weak symmetry stress-displacement-rotation formulation to the case where the stress tensor is not symmetric. The new weak formulation can be viewed as a perturbation of the stress-displacement-rotation formulation, and we characterize the stability of this formulation with respect to the elastic and mixing parameters.

The organization of this paper is as follows. The governing equations of a gel are reviewed and the total free energy assumptions are discussed in section 2. The minimization of the energy problem and the existence of minimizers are considered in section 3. In section 4, the Euler–Lagrange equations are derived, and linearizations of these are stated for further study in section 5. There, we first discuss the stability of the resulting displacement-pressure and the stress-displacement-rotation formulations with regard to the gel material parameters. The main component of section 5, though, is the derivation and analysis of a novel variation of the stress-displacement-rotation formulation. In section 6, we investigate the new formulation numerically, and then provide simulations of a confined polymer gel representing an artificial bone implant.

2. Governing equations of a gel. This paper focuses on the static equilibrium equations of a biphasic gel. In order to frame these equations and to introduce notation, we begin by presenting a brief overview of a model of gel dynamics and its derivation. This material is mostly classical, and we refer to [23, 28] and [8, 33] for a more thorough exposition. Under certain additional assumptions, the model reduces to the stress-diffusion coupling model proposed by Yamaue and Doi [30]. Next, assumptions regarding the total free energy of the gel, and hence the constitutive equations, are discussed. Adopting the viewpoint of Flory [15] and subsequent modelling approaches [8], we consider the sum of an elastic and a Flory–Huggins energy. These two terms account for the elasticity of the gel and the mixing of the polymer and solvent, respectively.

2.1. Governing equations of a biphasic gel. We follow the approach of [8], in which a model for gel dynamics is derived using mixture theory for a two-component system. As in [8], we consider the gel to be an immiscible, incompressible mixture of polymer and solvent. In an immiscible polymer-solvent mixture, the constitutive equations explicitly depend on the volume fractions ϕ_1 and ϕ_2 of the polymer and solvent, respectively. The volume fraction ϕ_i of each component is canonically defined as the volume of the component per unit volume of the gel. We denote by ρ_i the *mass* density of component i per unit volume in space for $i = 1, 2$. These are related to the *intrinsic* densities γ_i by $\rho_i = \gamma_i \phi_i$. A mixture is incompressible if the intrinsic density of each component is constant. Without loss of generality, we take the intrinsic densities of polymer and solvent to be equal to 1, and thus the mass density and

volume fraction of each component coincide. The incompressibility of the mixture constraint is therefore

$$\phi_1 + \phi_2 = 1. \tag{2.1}$$

Due to (2.1), the volume fraction of the solvent can be trivially eliminated in terms of the volume fraction of the polymer: $\phi_2 = 1 - \phi_1$. Hereafter, we omit the subscript and let $\phi = \phi_1$. We point out that the incompressibility of the mixture does not preclude deformations with change of volume. This point will be discussed further. Finally, we assume that there are neither voids nor additional material components in the system.

Let $\Omega \subset \mathbb{R}^n$ $(n = 1, 2, 3)$ denote a reference domain, with coordinates X, and assume that Ω is open and bounded with boundary $\partial\Omega$. Let

$$x : \Omega \to \Omega_x$$

denote a smooth deformation map satisfying $\det \nabla x > 0$. Ω_x denotes the deformed domain. Throughout this work, $F = \nabla x$ denotes the gradient of deformation. The divergence operator, taken row-wise when applied to matrices, is labeled div.

As governing equations, we will consider the equilibrium states of the model of gel dynamics described in [8]. These equations describe the balance of mass and linear momentum for the fluid and polymer components. The total Cauchy stress $\mathcal{T}$ for the gel dynamics model is defined as $\mathcal{T} = \phi\mathcal{T}_1 + (1 - \phi)\mathcal{T}_2$, where $\mathcal{T}_i$, $i = 1, 2$, are the individual Cauchy stresses for the polymer and solvent, respectively. For dynamic problems, the stress $\mathcal{T}$ contains elastic, mixing, and dissipative contributions from both the polymer and the solvent components. In equilibrium, only the elastic contribution from the polymer and the combined mixing pressure of the polymer and solvent contribute to the stress. The equilibrium situation is the case of interest in our study.

The static nature of this case renders it convenient to formulate the problem in terms of the first Piola–Kirchhoff stress tensor $\mathcal{S}$ over a reference domain. The first Piola–Kirchhoff stress can be obtained from the Cauchy stress: $\mathcal{S} = (\det F)\mathcal{T}F^{-T}$. The static equilibrium equation in the reference domain is obtained from the balance of linear momentum and reads

$$\operatorname{div} \mathcal{S}(F, \phi) = 0 \quad \text{in } \Omega. \tag{2.2}$$

We have made here, and will make throughout, an abuse of notation by labeling $\phi(X) := \phi \circ x(X)$ for $X \in \Omega$. The boundary conditions for the system are formulated as mixed displacement-traction conditions for the gel. For a more thorough exposition on the governing equations, boundary conditions, and the derivation of the model in general, we again refer to [8].

Assume next that the body in the reference configuration has a reference polymer volume fraction, $\phi_I : \Omega \to [0, 1]$. The quantity ϕ_I is the volume fraction of polymer present within the gel in its initial configuration. If ϕ_I is close to 0, then the gel is very fluid; conversely, if ϕ_I is close to 1, then the gel is very solid. Due to the incompressibility constraint in (2.1), the solvent volume fraction in the reference configuration is simply $1 - \phi_I$. In the gel problems we consider, the equilibrium state corresponds to a certain value of ϕ_I. When ϕ_I differs from the value corresponding to the gel equilibrium state, a *residual stress* is introduced into the system. This point will become relevant in later analysis.

Under the previous assumptions, the reference domain formulation of balance of mass reads

$$\int_\Omega \phi_I \,\mathrm{d}X = \int_{\Omega_x} \phi \,\mathrm{d}x = \int_\Omega \phi \det F \,\mathrm{d}X.$$

With the assumption that the above constraint is satisfied for all parts of the body Ω, we obtain the following local constraint:

$$\phi \det F = \phi_I \quad \text{in } \Omega. \tag{2.3}$$

Note that if $\det F = 1$, then $\phi_I = \phi$, so that no changes in the volume of the gel corresponds to no changes in volume fraction.

Remark 2.1. We emphasize that the balance of mass constraint (2.3) allows deformations with change in volume. In this regard, the mixture incompressibility assumption differs from classical incompressibility assumptions. Further, by definition, ϕ_I must take values in $[0, 1]$. This observation, in combination with (2.3), yields the constraint $\det F \geq \phi_I$.

2.2. Elastic and mixing energies. To provide a complete physical description of the gel, the governing equations in equilibrium, (2.2) and (2.3), must be augmented with appropriate constitutive equations for the polymer-solvent mixture. In this exposition, following [33], we shall assume that the gel is hyperelastic and model the total free energy for the gel as a sum of an elastic and a Flory–Huggins mixing energy [15].

Our approach aims to account for the osmotic pressure contributions from the elasticity of the polymer network and the chemistry of polymer and solvent mixing. The mechanics of the gel are accounted for by the elastic energy. The chemical features of the gel are accounted for by the Flory–Huggins mixing energy. The Flory–Huggins mixing theory quantifies the hydrophobic and hydrophilic molecular interactions within the gel. Hydrophilic interactions occur when there exists attraction between the polymer and the solvent, whereas hydrophobic interactions occur otherwise. In the former case, the polymer and solvent mix to form a gel; in the latter case, the repulsion between the polymer and solvent collapses the gel network on itself [19, 24]. The Flory–Huggins energy also accounts for phase transitions of the gel. Physically, gel phase transitions occur when the physical parameters reach a critical threshold, and the gel separates into phases. Mathematically, the gel phase transition is represented by a convexity transition of the total free energy. The Flory–Huggins energy allows for such a transition, given a set of critical parameter values.

The elastic energy per unit undeformed volume, denoted $\mathcal{W}_E$, is naturally formulated over the reference domain Ω. However, the Flory–Huggins energy, denoted $\mathcal{W}_{FH}$, is traditionally formulated per unit deformed volume [15]. This necessitates a change of variables on the Flory–Huggins energy. The resulting total free energy $\mathcal{E}$ now follows:

$$\mathcal{E}(x, \phi) = \int_\Omega \left(\mathcal{W}_E(F, \phi) + \det F \left(\mathcal{W}_{FH}(\phi) + c_{FH}\right)\right) \mathrm{d}X, \tag{2.4}$$

where c_{FH} is a nonnegative constant. We postpone discussion of the term $c_{FH}(\det F)$ momentarily, and instead provide some discussion of assumptions on the energy potentials $\mathcal{W}_E$ and $\mathcal{W}_{FH}$.

For elastic energy potentials, we restrict our attention to potentials of the form

$$\mathcal{W}_E(F, \phi) = \phi_I \,\mathcal{W}_P(F), \tag{2.5}$$

where the potential is separable in its arguments and depends linearly on the reference volume fraction. We observe that, as a consequence of the local balance of mass (2.3), the dependency on the reference volume fraction in the energy per undeformed volume naturally translates to a dependency on the volume fraction in the energy per deformed volume. This restriction is thus in accordance with that of [33]. In section 4 and onwards, we consider $\mathcal{W}_P$ taking the following, isotropic form:

$$\mathcal{W}_P(F) = \mu_E \left(\frac{1}{2p} \left(||F||^{2p} - ||I||^{2p} \right) + \frac{||I||^{2(p-1)}}{\beta} ((\det F)^{-\beta} - 1) \right) \tag{2.6}$$

for $p \geq 1$, where $||F||^2 = \operatorname{tr}(FF^T) = F : F$, I is the identity matrix in $\mathbb{R}^{n \times n}$, μ_E is an elastic stiffness modulus, and β a parameter related to polymer compressibility. The constants are such that the identity state has zero energy and is also stress-free. This elastic energy density (2.6) has been proposed and studied in the context of compressible elasticity (see [26], and the discussion in [9, section 4.10]). Note that the energy potential reduces to a compressible neo-Hookean potential when $p = 1$.

Remark 2.2. In view of Remark 2.1, the traditional interpretation of the term $(\det F)^{-\beta}$ does not apply within the mixture framework. In particular, the interpretation of the limiting case $\beta \to \infty$ is less clear. In the following, we shall view this term as a contraction penalty, ensuring that the domain does not degenerate to zero volume under deformation.

The Flory–Huggins mixing energy quantifies the energy available in the gel for polymer-solvent mixing, and the energy per deformed volume reads

$$\mathcal{W}_{FH}(\phi) = a\phi \ln \phi + b(1-\phi) \ln (1-\phi) + c\phi(1-\phi), \tag{2.7}$$

for positive, homogeneous parameters a, b, and c. The parameters a, b, and c can be related to the specific polymer, solvent, and gel environment as

$$a = \frac{K_B T}{V_m N_1}, \quad b = \frac{K_B T}{V_m N_2}, \quad c = \frac{K_B T \chi}{2V_m}, \quad \chi = \frac{\Delta w}{K_B T}, \tag{2.8}$$

where T is the absolute temperature, K_B is the Boltzmann constant, χ is the Flory interaction parameter, Δw is the change in energy per monomer-solvent interaction, V_m is the volume occupied by one monomer, and N_1 and N_2 are the number of lattice sites occupied by the polymer and solvent, respectively. Derivations for the Flory–Huggins energy and the interaction parameter χ can be found in [24, (4.21) and (4.23)], as well as in [8, 16, 19]. Note that the energy potential given by (2.7) is well defined for $\phi \in (0, 1)$. In addition, $\lim_{\phi \to 0^+} \mathcal{W}_{FH}(\phi) = \lim_{\phi \to 1^-} \mathcal{W}_{FH}(\phi) = 0$, and $\mathcal{W}_{FH}$ is smooth for $\phi \in (0, 1)$.

We return to a discussion of the coefficient c_{FH} in (2.4). The coefficient is defined as $c_{FH} = c_{FH}(a, b, c) = -\inf_{0<\phi<1} \mathcal{W}_{FH}(\phi)$, and it serves both a mathematical and a physical purpose. From a mathematical point of view, it ensures a lower bound of the total free energy in (2.4). This is necessary, since the energy given by (2.7) can take both positive and negative values, and a lower bound may not exist after the change of variables. We note that c_{FH} is clearly bounded in terms of other Flory–Huggins parameters: $0 \leq c_{FH} \leq (a+b)$. The $(\det F)$ factor comes from the change of variables from the deformed to the reference domain. Thus, $c_{FH}(\det F)$ results from combining energies from different frames, i.e., the elastic on the reference domain and the Flory–Huggins on the deformed domain. Although the origin of $c_{FH}(\det F)$ is slightly novel, restrictions on the growth of $(\det F)$ such as this are standard in elasticity theory [9].

Indeed, from a physical point of view, the presence of a factor of $(\det F)$ penalizes the volume changes in the gel.

The convexity of $\mathcal{W}_{FH}$, or the lack of such, plays a central role in the following analysis. Changes in the convexity of $\mathcal{W}_{FH}$ may impact the polyconvexity of the total free energy potential. Furthermore, changes in the polyconvexity of the total free energy potential impact the existence of energy minimizers. The convexity of $\mathcal{W}_{FH}$ depends on the values of the coefficients a, b, and c, and, in particular, on the interaction parameter χ. It can easily be seen that W_{FH} will be convex at ϕ if a, b, and c are such that

$$\frac{a}{\phi} + \frac{b}{1-\phi} \geq 2c.$$

Our final observation is that the constraint (2.3) allows for the elimination of ϕ in terms of $\det F$. This substitution reduces the total free energy to an entirely mechanical energy with the following potential:

$$\mathcal{E}(x) = \int_\Omega \mathcal{W}_E(F, \phi_I(\det F)^{-1}) + (\det F)\left(\mathcal{W}_{FH}(\phi_I(\det F)^{-1}) + c_{FH}\right) \mathrm{d}X. \tag{2.9}$$

The problem of minimizing (2.9) can be viewed as a nonlinear, compressible elasticity problem. One advantage of this formulation is that known techniques provide a framework for its mathematical and numerical analysis.

3. Existence of minimizing deformations. The physical deformation x of a gel defined over the domain Ω will be a minimizer in some admissible function space of the energy (2.9) augmented by body and boundary forces, if such a minimizer exists. This section, in particular the main theorem, Theorem 3.2, treats the existence of energy minimizers in the polyconvex case. A remark on a strategy for the nonconvex case closes the section.

We begin by introducing some notation in order to define the space of admissible functions and for later use.

- Let Ω be an open, bounded subset of $\mathbb{R}^n$, with Lipschitz boundary $\partial\Omega$, and let $\partial\Omega = \partial\Omega_0 \cup \partial\Omega_1$ with $\partial\Omega_0 \cap \partial\Omega_1 = \emptyset$. Assume that $\partial\Omega_0$ has positive measure. The unit outward normal on $\partial\Omega$ is denoted n.
- We use the linear spaces of n vectors $\mathbb{V}$, $n \times n$ matrices $\mathbb{M}$, symmetric matrices $\mathbb{S}$, and skew-symmetric matrices $\mathbb{K}$. The inner product on $\mathbb{M}$ is denoted :, and $||\cdot||$ is the Frobenius norm. The adjugate of an invertible matrix F is denoted $\operatorname{adj} F$; that is, $\operatorname{adj} F = (\det F)F^{-1}$.
- Let $\{\iota_1, \iota_2, \iota_3\}$ denote the invariants of the left Cauchy–Green strain tensor FF^T. Recall that $\iota_1 = \operatorname{tr}(FF^T)$, $\iota_2 = \operatorname{tr}\operatorname{adj}(FF^T)$, and $\iota_3 = \det(FF^T)$.
- The space of p-integrable fields on Ω with values in X is denoted $L^p(\Omega; X)$ with inner product $\langle\cdot,\cdot\rangle$ and norm $||\cdot||_0$. For notational ease, we will frequently omit the domain and range.
- $W^{k,p}(\Omega; \mathbb{V})$ denotes the Sobolev space of vector fields in $L^p(\Omega; \mathbb{V})$ such that the kth derivatives exist in the distributional sense and belong to L^p. The associated norm is denoted by $||\cdot||_{k,p}$. For $p = 2$, we use the standard abbreviation $H^k = W^{k,2}$ with norm $||\cdot||_k$. Further, we let

$$W_0^{1,p}(\Omega; \mathbb{V}) = \{x \in W^{1,p}(\Omega; \mathbb{V}),\ x = 0 \text{ on } \partial\Omega_0\}.$$

Also, $H_0^1 = W_0^{1,2}$.

- The space of square-integrable matrix fields with square-integrable divergence (taken row-wise) is denoted $H(\mathrm{div}, \Omega; \mathbb{M})$. We also have the constrained space

$$H_0(\mathrm{div}, \Omega; \mathbb{M}) = \{\sigma \in H(\mathrm{div}, \Omega; \mathbb{M}),\ \sigma \cdot n|_{\partial\Omega_1} = 0\}.$$

Assume that $\phi_I \in L^\infty(\Omega; (0,1))$. For $2p > n$ and a prescribed boundary condition $x_0 \in W^{1,2p}(\Omega)$, we define the space of admissible vector fields $\mathcal{A}$ as follows:

$$\mathcal{A} = \{x : \Omega \to \mathbb{R}^n,\ x \in x_0 + W_0^{1,2p},\ \mathrm{adj}\,\nabla x \in L^{2q}(\Omega),\ \det \nabla x \geq \phi_I \text{ a.e. in } \Omega\}.$$

We shall assume that the space $\mathcal{A}$ is nonempty; more specifically, that the constraint on the deformation gradient determinant can be fulfilled under the given boundary condition x_0. Now consider the following isotropic energy density:

$$\mathcal{E}(x) = \int_\Omega \mathcal{W}(F)\,\mathrm{d}X = \int_\Omega (\mathcal{G}(\iota_1, \iota_2) + \mathcal{H}(\iota_3))\,\mathrm{d}X. \tag{3.1}$$

Clearly, the gel energy defined by (2.9) can be expressed as a special case of (3.1), using the following identifications:

$$\mathcal{G}(\iota_1, \iota_2) = \frac{\phi_I \mu_E}{2p}\left(\iota_1^p - ||I||^{2p}\right), \tag{3.2}$$

$$\mathcal{H}(\iota_3) = \begin{cases} \iota_3\left(\mathcal{W}_{FH}(\phi_I \iota_3^{-1}) + c_{FH}\right) + C(\iota_3^{-\beta} - 1), & \phi_I < \iota_3, \\ +\infty, & \text{otherwise}, \end{cases} \tag{3.3}$$

where $C = C(\beta, \mu_E, \phi_I, p)$ is (implicitly) defined by (2.6) and the Flory–Huggins energy has been extended to the real line.

Remark 3.1. If $\mathcal{W}_{FH}$ is convex, $\mathcal{H}''(\iota_3) > 0$ for all $\iota_3 \geq \phi_I$. However, $\mathcal{H}''(\iota_3) < 0$ for some $\iota_3 \geq \phi_I$ if the interaction parameter χ, defined in (2.8), is sufficiently large.

Moreover, we assume that there exist constants $A_1, A_2 > 0$, $B \geq 0$ (or, if $\mathcal{G}(\iota_1, \iota_2) = \mathcal{G}(\iota_1)$, $A_2 \geq 0$) and $p > \frac{n}{2}$, $q \geq \frac{p}{2p-1}$ such that $\mathcal{G}(\iota_1, \iota_2)$ satisfies the growth condition

$$\mathcal{G}(\iota_1, \iota_2) \geq A_1 \iota_1^p + A_2 {\iota_2}^q - B. \tag{3.4}$$

Clearly, (3.2) satisfies (3.4) with $A_2 = 0$ if $2p > n$ and $\mu_E > 0$. Note that the neo-Hookean potential, corresponding to $p = 1$, does not satisfy the growth condition for $n \geq 2$.

The existence of minimizers of the energy (3.1), with $\mathcal{H}$ convex, over the space of admissible vector fields $\mathcal{A}$ is established in Theorem 3.2 below. We note that the assumption that $\mathcal{G}$ and $\mathcal{H}$ are convex gives the polyconvexity of $\mathcal{W}$.

THEOREM 3.2. *Assume that $\mathcal{G}(\cdot, \cdot)$ is convex and satisfies the growth inequality* (3.4)*, and that $\mathcal{H}(\cdot)$ is convex. Suppose that $x_0 \in W^{1,2p}$ and that $\det \nabla x_0 > \phi_I$. Then there exists $x \in \mathcal{A}$ that minimizes the energy* (3.1).

Proof. We first observe that, by the construction of c_{FH}, there exists an $m > -\infty$ such that $m \equiv \inf_{\mathcal{A}} \mathcal{E}(x)$. Let $\{x_k\}_{k \geq 1} \in \mathcal{A}$ denote a minimizing sequence of $\mathcal{E}$; that is, $\{x_k\}$ has the property $\lim_{k\to\infty} \mathcal{E}(x_k) = m$. To show that the problem of minimizing $\mathcal{E}$ in the set $\mathcal{A}$ has a solution, we proceed along the following steps.

Step 1. Prove that there exists a subsequence of $\{x_k\}$ (still denoted by x_k) such that

$$\lim_{k\to\infty} x_k = \bar{x} \quad \text{weakly in } W^{1,2p}.$$

Step 2. Show that $\mathcal{E}$ is weakly lower semicontinuous in $W^{1,2p}$; that is, for any minimizing sequence $\{x_k\} \in \mathcal{A}$,

$$\lim_{k\to\infty} \inf \mathcal{E}(x_k) \geq m. \tag{3.5}$$

Step 3. Show that $\bar{x} \in \mathcal{A}$. This combined with the weak lower semicontinuity property (3.5) allows us to conclude that

$$\min_{y\in\mathcal{A}} \mathcal{E}(y) = \mathcal{E}(\bar{x}).$$

We outline Steps 1 and 2 following [9, Theorem 7.7.1] and [4]. First, we find a lower bound of the energy. It follows from (3.4) and the form of $\mathcal{H}$ that there exists a constant γ such that

$$\mathcal{E}(x) \geq \int_\Omega \left(A_1\|\nabla x\|^{2p} + A_2\|\operatorname{adj}\nabla x\|^{2q} + A_3(\det\nabla x)\right) \mathrm{d}X + \gamma|\Omega|$$

for all $x \in \mathcal{A}$. An application of the generalized Poincaré inequality [9, Theorem 6.1-8(b)] allows us to conclude that there exist constants $a_1 > 0$ and a_2 such that

$$\mathcal{E}(x) \geq a_1 \left(\|x\|^{2p}_{1,2p} + \|\operatorname{adj}\nabla x\|^{2q}_{0,2q}\right) + a_2 \tag{3.6}$$

for all $x \in \mathcal{A}$. In particular, it follows from (3.6) that the the sequence $\{x_k, \operatorname{adj}\nabla x_k\}$ is bounded in $W^{1,2p} \times L^{2q}$. By the assumptions on p and q, this space is reflexive. Therefore, there exists a subsequence $\{x_k, \operatorname{adj}\nabla x_k\}$ that converges weakly to an element $(\bar{x}, \operatorname{adj}\nabla\bar{x})$ in the space $W^{1,2p} \times L^{2q}$.

Second, by the weak lower semicontinuity of the determinant function, we have that

$$\det\nabla x_k \rightharpoonup \det\nabla\bar{x} \qquad \text{in } L^{\frac{2p}{n}}. \tag{3.7}$$

The weak lower semicontinuity of $\mathcal{E}$ is then a consequence of the convexity of $\mathcal{G}$ together with the convexity of $\mathcal{H}$.

Third, the property $\det\nabla\bar{x} \geq \phi_I$, a.e. in Ω, follows from Mazur's lemma together with (3.7). Indeed, by Mazur's lemma, for a given $\epsilon > 0$ there exists $N = N(\epsilon)$, and $\{\lambda_i(\epsilon)\}$ with $\sum_1^N \lambda_i = 1$, such that

$$\left\| \sum_1^N \lambda_i \det\nabla x_i - \det\nabla\bar{x} \right\|_{0,\frac{2p}{n}} < \epsilon.$$

Since $\det\nabla x_k \geq \phi_I$, we conclude that $\det\nabla\bar{x} \geq \phi_I$ almost everywhere, and hence $\bar{x} \in \mathcal{A}$. ∎

The relation $\phi = \phi_I(\det\nabla\bar{x})^{-1}$ allows us to recover the volume fraction variable $\phi \in L^\infty(\Omega)$, which corresponds to the energy minimizer $\bar{x}$.

Remark 3.3. In the case that $\mathcal{H}$ is nonconvex, the previous theorem does not apply. In such a case, the total free energy can be modified by the addition of a regularization term. The new gel energy becomes

$$\mathcal{E}_r(x,\phi) = \int_\Omega \mathcal{W}_E(F)\,\mathrm{d}X + \int_{\Omega_x} \left(\mathcal{W}_{FH}(\phi) + c_{FH} + \epsilon\,||\nabla_x\phi||^2\right)\mathrm{d}x, \tag{3.8}$$

with $\epsilon > 0$ small. Although we do not consider this extension in the remainder of this work, we point out that existence of a minimizer for a regularized energy of the form (3.8), although with a modified $\mathcal{W}_E$ and $\mathcal{W}_{FH}$, was studied in [32].

4. Linearizations of the Euler–Lagrange equations. With the existence of minimizers proven for the convex case, we turn our attention to the Euler–Lagrange equations. The equations are nonlinear, but we provide a linearization of the equations in this section. This is motivated by the fact that, for the biomedical applications we aim to consider in this exposition, the linear regime may be meaningful and applicable. Moreover, qualitative effects of changes in the environment can be studied through linearized perturbations. The resulting linear boundary value problem will be further studied in sections 5 and 6.

We consider the energy defined by (2.9), complemented by the energy potentials specified by (2.5), (2.6), and (2.7), and augmented by a body force g and a boundary stress s_0 on $\partial\Omega_1$. Upon taking variations, we obtain the Euler–Lagrange equilibrium equations over the reference domain Ω for the first Piola–Kirchhoff stress tensor $\mathcal{S}$; cf. (2.2). The strong form of the problem formally reads as follows: find a deformation $x : \Omega \to \Omega_x$ and the associated stress tensor $\mathcal{S}$ such that

$$\mathcal{S} = \nu(\nabla x)\,\nabla x - \kappa(\nabla x)\,\nabla x^{-T} \quad \text{in } \Omega, \tag{4.1a}$$

$$\operatorname{div}\mathcal{S} = g \quad \text{in } \Omega, \tag{4.1b}$$

$$x = x_0 \quad \text{on } \partial\Omega_0, \quad \mathcal{S}\cdot n = s_0 \quad \text{on } \partial\Omega_1, \tag{4.1c}$$

where n denotes the outward oriented normal of the boundary. The coefficients ν and κ are functions of a matrix variable and take the form

$$\begin{aligned} \nu(F) &= \mu_E \phi_I ||F||^{2(p-1)}, \\ \kappa(F) &= \mu_E \phi_I ||I||^{2(p-1)} (\det F)^{-\beta} - (\det F)\left(\mathcal{W}_{FH}(\phi) + c_{FH} - \phi \mathcal{W}'_{FH}(\phi)\right). \end{aligned} \tag{4.2}$$

Here, we have reintroduced $\phi = \phi_I (\det F)^{-1}$ for the sake of notational brevity. Recall that $\mu_E > 0$, β, and $p \geq 1$ are elastic parameters, the former being the elastic shear modulus. As before, ϕ_I is the volume fraction in the reference configuration. The derivative of the Flory–Huggins potential $\mathcal{W}'_{FH}$ is the derivative with respect to the variable ϕ; cf. (2.7).

For frequent later reference, we label the residual stress (at $F = I$)

$$r(\phi) = \mathcal{W}_{FH}(\phi) + c_{FH} - \phi \mathcal{W}'_{FH}(\phi). \tag{4.3}$$

This quantity plays a key role in the numerical methods to follow. The residual stress is the stress in the reference state defined by the reference domain. For purely elastic materials, the residual stress is often assumed to vanish. In our model, the notion of vanishing residual stress becomes a restriction on the reference volume fraction ϕ_I, since the residual stress will vanish if and only if ϕ_I satisfies $r(\phi_I) = 0$. The existence of such ϕ_I is guaranteed by the lifting of the Flory–Huggins potential by c_{FH}. If ϕ_I is a global minimizer of the Flory–Huggins potential, $\mathcal{W}_{FH}(\phi_I) = -c_{FH}$ and $\mathcal{W}'_{FH}(\phi_I) = 0$, which thereby results in $r(\phi_I) = 0$. However, this constraint is too limiting for our purposes, as the volume fraction in the reference configuration may be arbitrary. We therefore also aim to consider ϕ_I such that $r(\phi_I) \neq 0$. In fact, this is a key point for the following.

4.1. The linearized boundary value problem. The Flory–Huggins energy potential $\mathcal{W}_{FH}$, and hence the constitutive equations of (4.1), depend on the physical parameters $\{a, b, c\}$. In the form given by (2.8), these parameters are explicitly dependent on the temperature but may also be sensitive to other environmental parameters. In order to obtain a qualitative understanding of the effect of changes in the environment, perturbations of a generic environment parameter T may be considered.

Let the Piola–Kirchhoff stress tensor $\mathcal{S} = \mathcal{S}(F, T)$ be as defined by (4.1a). Assuming that $F = \nabla(x_0 + u)$ and $T = T_0 + \Delta T$, give the first order approximation

$$\mathcal{S}(F,T) \approx \mathcal{S}(F_0,T_0) + \frac{\partial \mathcal{S}}{\partial F}(F_0,T_0)[\nabla u] + \frac{\partial \mathcal{S}}{\partial T}(F_0,T_0)[\Delta T], \tag{4.4}$$

where $F_0 = \nabla x_0$. The approximation is valid under the assumption of small perturbations in the deformation gradient and the environment parameter. On the right-hand side, the first term corresponds to the force induced by the residual stress at (F_0, T_0), the second term is the elasticity tensor linearized about the deformation gradient F_0, and the third term corresponds to the force induced by the change of environment. If $\Delta T = 0$ and $F_0 = I$, (4.4) reduces to the linear elasticity approximation. A set of elementary but somewhat lengthy calculations gives the following expression of the Gateaux derivative of $\mathcal{S}$:

$$\begin{aligned}\frac{\partial \mathcal{S}}{\partial F}(F_0)[G] = \nu(F_0)G + \kappa(F_0)F_0^{-T}G^TF_0^{-T} \\ + \lambda_0(F_0)(F_0 : G)F_0 + \lambda_1(F_0)(F_0^{-T} : G)F_0^{-T},\end{aligned} \tag{4.5}$$

where ν and κ are defined by (4.2). The constants λ_0 and λ_1 are defined by

$$\begin{aligned}\lambda_0(F) &= 2(p-1)\mu_E\phi_I||F||^{2(p-2)}, \\ \lambda_1(F) &= \mu_E\phi_I\beta||I||^{2(p-1)}(\det F)^{-\beta} + (\det F)(r(\phi) + \phi^2\mathcal{W}''_{FH}(\phi)),\end{aligned} \tag{4.6}$$

where, once again, we write $\phi = \phi_I(\det F)^{-1}$ and r is defined by (4.3).

We take a closer look at the residual stress at a given deformation gradient F_0. Since the constitutive relation is isotropic, $\mathcal{S}(F_0, \cdot) = 0$ implies that $F_0 = f_0 I$ for some scalar f_0. In other words, for the residual stress at F_0 to vanish, F_0 must be a certain pure expansion or contraction. Furthermore, we note that for any such $f_0 I$, the forcing terms of (4.4) correspond to pure pressures. In the case $f_0 = 1$, $\mathcal{S}(I, \cdot) = r(\phi_I)I$, where $r(\phi_I)$ is defined by (4.3). The linear boundary value problem resulting from taking $f_0 = 1$ is summarized below in Problem 1.

PROBLEM 1. *Let Ω be an open and bounded domain in $\mathbb{R}^n$ with Lipschitz boundary $\partial\Omega = \partial\Omega_0 \cup \partial\Omega_1$, $\partial\Omega_0 \cap \partial\Omega_1 = \emptyset$. For a given $\phi_I : \Omega \to (0,1)$ and given forces f and g, find the displacement $u : \Omega \to \mathbb{V}$ and the stress tensor $\sigma : \Omega \to \mathbb{M}$ satisfying the boundary conditions $u|_{\partial\Omega_0} = u_0$ and $\sigma \cdot n|_{\partial\Omega_1} = s_0$ and such that*

$$\sigma - C_r[\nabla u] = r(\phi_I)I + f, \tag{4.7a}$$

$$\operatorname{div}\sigma = g. \tag{4.7b}$$

Here, r is defined by (4.3) *and C_r is the residual-dependent stiffness tensor,*

$$C_r[\nabla u] = \frac{\partial \mathcal{S}}{\partial F}(I)[\nabla u] = \mu(\phi_I)\nabla u + (\mu(\phi_I) - r(\phi_I))\nabla u^T + \lambda(\phi_I)(\operatorname{div} u)\, I, \tag{4.8}$$

and the generalized Lamé coefficients μ and λ are given by

$$\begin{aligned}\mu(\phi) &= \mu_E\phi||I||^{2(p-1)}, \\ \lambda(\phi) &= 2(p-1)\mu_E\phi||I||^{2(p-2)} + \beta\mu_E\phi||I||^{2(p-1)} + r(\phi) + \phi^2\mathcal{W}''_{FH}(\phi).\end{aligned} \tag{4.9}$$

If ϕ_I is such that $r = r(\phi_I) = 0$, the stiffness operator C_r reduces to the standard linear elasticity tensor, although the Lamé coefficients μ and λ additionally depend

on the reference volume fraction ϕ_I and the Flory–Huggins potential $\mathcal{W}_{FH}$. In this case, the stress tensor is symmetric; that is, $\sigma : \Omega \to \mathbb{S}$. On the other hand, if ϕ_I is such that $r(\phi_I) \neq 0$, then the reference volume fraction is not an equilibrium volume fraction, and the gel is inclined to deform by either swelling or collapsing. We consider two possible approaches to this case and preface their description by noting that both approaches allow us to arbitrarily prescribe a reference volume fraction ϕ_I.

The first approach is simply to consider the system of equations (4.7) directly. However, the additional source introduced by the residual stress and, more importantly, the skew-symmetry part of the displacement gradient must be resolved. This approach is studied carefully in the main part of section 5.

The second approach is restricted to the case where the material parameters are assumed to be homogeneous. In this approach, we can consider linearizations about homogeneous, nonidentity deformations $F_0 = f_0 I$, where $f_0 \neq 1$. These deformations are pure expansions or contractions with f_0 chosen such that (4.1a) vanishes; that is, $\mathcal{S}(f_0 I, \cdot) = 0$. The stipulation is that f_0 is such that

$$\nu(f_0 I) f_0 - \kappa(f_0 I) f_0^{-1} = 0. \tag{4.10}$$

The linearized equations, resulting from considering (4.4) and (4.5) with $F_0 = f_0 I$, become (4.7) and (4.8) with $r = 0$ and the Lamé coefficients

$$\mu(\phi, f_0) = \nu(f_0 I), \quad \lambda(\phi, f_0) = f_0^2 \lambda_0(f_0 I) + f_0^{-2} \lambda_1(f_0 I), \tag{4.11}$$

where λ_0, λ_1 are given by (4.6). In addition, we observe that the linearization about a nonidentity state may require some additional care when applying boundary conditions, but we postpone further discussion of this until section 6.

Having set up the equations to study, we continue by discussing weak formulations and discretizations of Problem 1 and the linear stability of such in terms of the gel parameters, paying special attention to the role of residual stress r. We shall demonstrate the use of both the approaches described above in the subsequent sections, but will explicitly state when we consider (4.11) in place of (4.9).

5. Weak formulations and linear stability. The boundary value problem defined by Problem 1 with $r = 0$ is, in effect, the standard linear elasticity problem. Finite element and mixed finite element methods for the approximation of these equations are very well understood, and a multitude of approaches are available. In this work, we consider mixed finite elements, a choice which is motivated by two primary considerations. First, it is well known that the pure displacement formulation, which results from eliminating the stress tensor σ and looking for a displacement $u \in H^1(\Omega; \mathbb{V})$, is unreliable if $\lambda \to \infty$ or if the clamped boundary $\partial\Omega_0$ constitutes only a small part of the total boundary [5]. In our problem, since $\lambda(\phi_I) \to \infty$ as $\phi_I \to 1$ for λ defined by (4.9), we seek weak formulations that are robust in the sense that they afford uniform convergence in the coefficient λ. Mixed finite element methods offer such a feature. Second, in the biomedical confinement problems we address in this paper, the quantity of main interest is the stress $\sigma \cdot n$. Therefore, it may be natural to approximate this variable directly. A recent survey of mixed finite element methods for linear elasticity was presented by Falk [12].

In this section, we shall examine two types of mixed finite element methods for the gel equations as defined by Problem 1: the *displacement-pressure* and *stress-displacement-rotation* formulations. Both are robust with respect to the coefficient λ and typically give second- (or higher) order stress approximations for smooth solutions. Both will be used for simulations in section 6. In the displacement-pressure

method, the displacement u and a pressure p are approximated directly. This formulation gives a version of the Stokes equations with an additional stabilization term. The discrete stability requirements on the associated pair of finite element spaces typically mandate higher order approximation spaces for the displacement. This, in turn, induces higher order approximations for the stresses. The second method, the stress-displacement-rotation formulation, approximates the stress, the displacement, and the rotation (the skew-symmetric part of the displacement gradient). Here the stress is approximated as the primal variable and therefore typically has a higher order accuracy than the displacement.

Both types of mixed finite element methods have been thoroughly studied from the linear elasticity viewpoint, and we refer to [5, 12] for a thorough treatment. We emphasize, however, that the case where $r \neq 0$ requires additional care. The main results in this section address the stress-displacement-rotation formulation in that setting.

5.1. Weak formulations for vanishing residual stress. We now state the two mixed formulations applied to the boundary value problem defined by Problem 1 with $r = 0$ and discuss the linear stability requirements placed on the gel parameters. The case $r \neq 0$ will be considered in the subsequent sections. For the sake of clarity, we assume that the boundary conditions are homogeneous: $u_0 = 0$ on $\partial\Omega_0$, $s_0 = 0$ on $\partial\Omega_1$. The notation is as introduced in section 3.

We begin with a discussion of the displacement-pressure formulation. Introducing a pressure $p = \lambda \operatorname{div} u$, one easily obtains the following weak displacement-pressure formulation of (4.7). Given $f \in L^2(\Omega; \mathbb{S})$ and $g \in L^2(\Omega; \mathbb{V})$, find $u \in H_0^1(\Omega; \mathbb{V})$ and $p \in L^2(\Omega)$ such that

$$\begin{aligned} \langle 2\mu\varepsilon(u), \varepsilon(v)\rangle + \langle p, \operatorname{div} v\rangle &= -\langle f, \nabla v\rangle - \langle g, v\rangle \quad \forall\, v \in H_0^1(\Omega; \mathbb{V}), \\ \langle \operatorname{div} u, q\rangle - \langle \lambda^{-1} p, q\rangle &= 0 \quad \forall\, q \in L^2(\Omega), \end{aligned} \tag{5.1}$$

where ε is the symmetrized gradient and $\mu = \mu(\phi_I)$ and $\lambda = \lambda(\phi_I)$ are as defined in (4.9). The robustness in the limit $\lambda \to \infty$ is due to the fact that (5.1) are the Stokes equations in the limit $\lambda = \infty$. Furthermore, if $\mu > 0$ and $2\mu + n\lambda > 0$, there exist stable solutions u and p to (5.1).

The dependencies in the Lamé coefficients on the parameters of the problem have implications for the stability of the method. Notice that $\phi_I^2 \mathcal{W}''_{FH}(\phi_I) \to \infty$ corresponds to $\lambda \to \infty$. The robustness in λ may therefore be important if ϕ_I is close to 1 (or 0), that is, if the gel is almost dry (or almost fluid) in the reference configuration. It is clear that $\mu(\phi_I) > 0$ when defined by (4.9). In addition, $\lambda > 0$ if the Flory–Huggins energy potential $\mathcal{W}_{FH}$ is convex. If $\mathcal{W}_{FH}$ is sufficiently nonconvex, λ may take negative values, and consequently the gel may display auxetic behavior. It also follows that the condition $2\mu + n\lambda > 0$ can break only if $\mathcal{W}_{FH}$ is sufficiently nonconvex. If one instead considers the Lamé parameters obtained by a linearization about a nonidentity state (cf. (4.11)), similar considerations apply. However, we see from (4.11) and (4.6) that λ might take negative values, even if $\mathcal{W}_{FH}$ is convex.

The alternative approach, the stress-displacement-rotation formulation, approximates the stress tensor σ and the displacement u separately while weakly enforcing the symmetry of the stress tensor. The rotation γ enters as a Lagrange multiplier corresponding to the latter symmetry constraint, and it is easily seen that $\gamma = \operatorname{skw} \nabla u$, where

$$2 \operatorname{skw} \tau = \tau - \tau^T.$$

The corresponding weak formulation of (4.7) with $r = 0$ reads as follows. Given $f \in L^2(\Omega; \mathbb{S})$ and $g \in L^2(\Omega; \mathbb{V})$, find $\sigma \in H_0(\operatorname{div}, \Omega; \mathbb{M})$, $u \in L^2(\Omega; \mathbb{V})$, and $\gamma \in L^2(\Omega; \mathbb{K})$ satisfying

$$\begin{aligned} \langle A_0\sigma, \tau\rangle + \langle \operatorname{div}\tau, u\rangle + \langle \tau, \gamma\rangle &= \langle A_0 f, \tau\rangle \qquad \forall\, \tau \in H_0(\operatorname{div}, \Omega; \mathbb{M}), \\ \langle \operatorname{div}\sigma, v\rangle + \langle \sigma, \eta\rangle &= \langle g, v\rangle \quad \forall\, v \in L^2(\Omega; \mathbb{V}),\ \eta \in L^2(\Omega; \mathbb{K}). \end{aligned} \tag{5.2}$$

Here A_0 is the compliance tensor, given as the inverse of the stiffness tensor C_0:

$$A_0\tau = \frac{1}{2\mu}\left(\tau - \frac{\lambda}{2\mu + n\lambda}\operatorname{tr}\tau\right), \tag{5.3}$$

with $\mu = \mu(\phi_I)$ and $\lambda = \lambda(\phi_I)$, as before. Similar considerations for the existence of stability of solutions with regard to the gel material parameters apply, as for the displacement-pressure formulation. In particular, A will not be uniformly bounded as $2\mu + n\lambda \to 0$. We remark that the symmetry of the stress tensor could also be enforced strongly, in the sense that the stress tensor function space could be restricted to the symmetric matrix fields [3]. However, as we shall see in the following, the weak symmetry approach lends itself more easily to the nearly symmetric case.

5.2. Weak formulations incorporating residual stress. The above systems (5.1) and (5.2) illustrate that the weak formulations for the small-strain gel equations are entirely analogous to the weak formulations for the standard linear elasticity equations in the case where the residual stress vanishes. However, if the residual stress does not vanish, the skew-symmetric part of the displacement gradient and an additional source will enter the equations; cf. (4.8). In particular, the stress tensor will *not* be symmetric. The displacement-pressure formulation (5.1) can easily be extended to this case. One may introduce a pressure $p = \lambda \operatorname{div} u$ as before and, instead of the symmetrized gradient, consider the displacement gradient and its transpose separately. However, the stress-displacement-rotation formulation requires more attention. In this section, we shall demonstrate how the stress-displacement-rotation formulation (5.2) can be extended to deal with a nearly symmetric stress tensor. To the authors' knowledge, this is an original approach. Accordingly, the derivation is presented in some detail.

The derivation of the stress-displacement-rotation formulation of (5.2) relies on both the symmetry of the stress tensor and the inversion of the stress-strain relation. Thus, traditionally, the symmetry of the stress tensor is a key factor. In the case $r \neq 0$, the stress tensor is not symmetric. However, the form of the stiffness tensor C and the premise that f takes symmetric values give a restriction on the skew component of the stress tensor. More specifically, the skew component of the stress tensor is proportional to the skew-symmetric part of the displacement gradient:

$$\operatorname{skw}(\sigma) = r \operatorname{skw}(\nabla u) = r\gamma. \tag{5.4}$$

We note that if $r = 0$, this reduces to the classical symmetry constraint for the stress tensor.

The inversion of the stress-strain relation follows the standard procedure. From (4.8), we find that

$$\operatorname{tr}\varepsilon(u) = \frac{1}{\zeta_r}\left(\operatorname{tr}\sigma - nr - \operatorname{tr} f\right), \quad \zeta_r = 2\mu + n\lambda - r. \tag{5.5}$$

This relation allows us to eliminate $\operatorname{tr}\varepsilon$ in terms of $\operatorname{tr}\sigma$. Assuming that $2\mu - r \neq 0$, we introduce the residual-dependent compliance tensor A_r:

$$A_r\sigma = \frac{1}{2\mu - r}\left(\sigma - \frac{\lambda}{\zeta_r}\operatorname{tr}\sigma I\right).$$

Further, let $\gamma = \operatorname{skw}(\nabla u)$ and recall that $\varepsilon(u) = \nabla u - \gamma$. The stress-strain relation follows,

$$A_r\sigma = \nabla u - k_r\gamma + A_r\left(rI + f\right), \quad k_r = 1 - \frac{r}{2\mu - r}. \tag{5.6}$$

Multiplying (5.6), (4.7b), and (5.4) by fields τ, v, and η, respectively, and integrating the ∇u term by parts give the following *nearly symmetric* weak formulation:

$$\begin{aligned} &\langle A_r\sigma, \tau\rangle + \langle \operatorname{div}\tau, u\rangle + \langle k_r\tau, \gamma\rangle = \langle A_r(rI + f), \tau\rangle \quad \forall\, \tau \in H_0(\operatorname{div}, \Omega; \mathbb{M}), \\ &\langle \operatorname{div}\sigma, v\rangle + \langle k_r\sigma, \eta\rangle - \langle rk_r\gamma, \eta\rangle = \langle g, v\rangle \quad \forall\, v \in L^2(\Omega; \mathbb{V}),\ \eta \in L^2(\Omega; \mathbb{K}). \end{aligned} \tag{5.7}$$

The relation (5.4) has been multiplied by the factor k_r for the sake of the symmetry of the system of equations. Observe that $A_r(rI) = r\zeta_r^{-1}I$, where ζ_r is given by (5.5). System (5.7) can be written in the following, strong form:

$$\begin{pmatrix} A_r & -\nabla & k_rI \\ \operatorname{div} & 0 & 0 \\ k_r\operatorname{skw} & 0 & -rk_r \end{pmatrix} \begin{pmatrix} \sigma \\ u \\ \gamma \end{pmatrix} = \begin{pmatrix} A_r(rI + f) \\ g \\ 0 \end{pmatrix}. \tag{5.8}$$

Finally, we remark that if $r = 0$, then $k_r = 1$ and $rk_r = 0$. Thus, comparing (5.7) to (5.2), we see that the nearly symmetric formulation reduces to the weakly symmetric formulation in that case. We also note that $k_r \in (0, 2)$ when $r \in (-\infty, \mu)$.

5.3. Stability of nearly symmetric stress-displacement formulation. We now inspect the linear stability of the nearly symmetric formulation (5.7), paying special attention to r. The case $r = 0$ has already been discussed. For $r \neq 0$, it is easy to see from (5.8) that the system of equations takes the form of a saddle point problem with an additional perturbation term. Therefore, this formulation also naturally lends itself to analysis using the Brezzi theory of saddle point problems and its extensions to perturbed saddle point problems [7]. However, we note that, in contrast to the standard perturbed case, the parameter r affects virtually all terms of (5.8).

The range of values for r for which system (5.7) has a stable solution is discussed in Lemma 5.1 and Theorem 5.2. The lemma gives an upper bound on the residual r in terms of the parameters μ and λ, such that the saddle point part of (5.7) satisfies the classical Brezzi conditions. However, the $\langle rk_r\gamma, \eta\rangle$ term of (5.7) will act as a destabilizer for $r < 0$. As this case simply corresponds to a negative residual stress, it is indeed relevant for the current exposition. Thus, we are also interested in a negative lower bound. Theorem 5.2 makes these notions more precise. The case $f, g = 0$ and the assumption of homogeneous elastic and mixing parameters are considered for the sake of simplicity.

LEMMA 5.1. *For $\mu > 0$ and $\lambda \in \mathbb{R}$, assume that $r < \min(\mu, 2\mu + n\lambda)$. Define*

$$Z_r = \{\tau \in H(\operatorname{div}, \Omega; \mathbb{M}),\ \langle \operatorname{div}\tau, v\rangle + \langle \kappa_r\tau, \eta\rangle = 0 \quad \forall\, v \in L^2(\Omega; \mathbb{V}),\ \eta \in L^2(\Omega; \mathbb{K})\}.$$

Then A_r is continuous and coercive on Z_r. In particular, there exist positive constants α_r, a_r such that

$$|\langle A_r\sigma,\tau\rangle| \le a_r||\sigma||_0||\tau||_0 \quad \forall\,\sigma,\tau \in H(\mathrm{div},\Omega;\mathbb{M}), \tag{5.9}$$

$$\langle A_r\tau,\tau\rangle \ge \alpha_r||\tau||_0^2 = \alpha_r||\tau||_{\mathrm{div}}^2 \quad \forall\,\tau \in Z_r. \tag{5.10}$$

Further, for any $v \in L^2(\Omega;\mathbb{V})$, $\eta \in L^2(\Omega;\mathbb{K})$, there exist a $\tau \in H_0(\mathrm{div},\Omega;\mathbb{M})$ and a $\beta > 0$, independent of r, such that

$$||\tau||_{\mathrm{div}}\left(||v||_0 + ||k_r\eta||_0\right) \le \beta\left(\langle \mathrm{div}\,\tau, v\rangle + \langle k_r\tau,\eta\rangle\right). \tag{5.11}$$

Proof. The proof of this lemma is just a minor modification of the proof for the case with $r = 0$, for instance the one given in [5, p. 308 ff]. We simply remark that it is evident that for $\tau \in Z_r$, $\mathrm{div}\,\tau = 0$. The bounds follow as usual, as the assumption $r < \mu$ in particular implies that $2\mu - r > 0$ and $k_r > 0$. ∎

THEOREM 5.2. *Let $\sigma \in H(\mathrm{div},\Omega;\mathbb{M})$, $u \in L^2(\Omega;\mathbb{V})$, and $\gamma \in L^2(\Omega;\mathbb{K})$ solve (5.7) with $f, g = 0$. Assume that μ, λ, and r are such that Lemma 5.1 holds. Additionally, if $r < 0$, assume that*

$$\alpha_r - \frac{|r|}{k_r}2\beta^2 a_r^2 > 0. \tag{5.12}$$

Then, there exists a constant $c > 0$ such that

$$||\sigma||_{\mathrm{div}}^2 \le c||rI||_0^2, \quad ||u||_0 + k_r||\gamma||_0 \le c(||\sigma||_0 + ||rI||_0). \tag{5.13}$$

Proof. For σ, u, γ solving (5.7),

$$\langle A_r\sigma,\sigma\rangle + \langle rk_r\gamma,\gamma\rangle = \langle A_r(rI),\sigma\rangle. \tag{5.14}$$

Under the assumption that r is such that Lemma 5.1 holds, (5.11) in combination with (5.9) gives

$$||u||_0 + |\kappa_r|||\gamma||_0 \le \beta a_r\left(||\sigma||_0 + ||rI||_0\right). \tag{5.15}$$

Hence, if $r \ge 0$, (5.14) immediately gives the stability bound (5.13). So, consider the case $r < 0$. Using (5.14), (5.15), and (5.10), we obtain

$$\left(\alpha_r - \frac{|r|}{k_r}2\beta^2 a_r^2\right)||\sigma||_0^2 \le \langle A_r(rI),\sigma\rangle + \frac{|r|}{k_r}2\beta^2 a_r^2||rI||_0^2,$$

giving rise to the condition (5.12). ∎

In essence, the inequality of (5.12) quantifies a value $r_0 < 0$ such that (5.13) holds for $r \in (r_0, \mu)$. With reference to (4.3), recall that $r = r(\phi_I)$ is induced by a given reference volume fraction ϕ_I and that μ and λ are given by (4.9). We note that the estimates of Lemma 5.1 and Theorem 5.2 degenerate as $r \to \mu$, $2\mu - r + n\lambda \to 0$, or in the limiting case of (5.12). Hence, the behavior in, and beyond, these limiting cases is not clear. This aspect will be investigated numerically in the next section. In particular, loss of stability is indeed detected for r sufficiently negative.

The approximation properties of a discretization of (5.7) now follow from the standard theory [7]. Let $\Sigma_h \subset H_0(\mathrm{div},\Omega;\mathbb{M})$, $V_h \subset L^2(\Omega;\mathbb{V})$, and $Q_h \subset L^2(\Omega;\mathbb{K})$ be finite-dimensional spaces associated with a simplicial tessellation $\mathcal{T}_h$ of Ω, h denoting the meshsize. Assume that $\Sigma_h \times V_h \times Q_h$ defines a stable discretization of (5.2); that

is, assume that (5.10) and (5.11), viewed over the discrete spaces, are satisfied with positive constants independent of h. Further, assume that the material parameters are such that Theorem 5.2 holds. Then, if $\sigma_h \in \Sigma_h$, $u_h \in V_h$, and $\gamma_h \in Q_h$ solve (5.7) for all $\tau \in \Sigma_h$, $v \in V_h$, and $\eta \in Q_h$, there exists $C > 0$ independent of h such that

$$||\sigma - \sigma_h||_{\mathrm{div}} + ||u - u_h||_0 + ||\gamma - \gamma_h||_0 \leq C \left(\inf_{\tau \in \Sigma_h} ||\sigma - \tau||_{\mathrm{div}} + \inf_{v \in V_h} ||u - v||_0 + \inf_{\eta \in Q_h} ||\gamma - \eta||_0 \right).$$

5.4. Choice of discretization spaces. We conclude this section with some considerations regarding specific discretizations of (5.1) and (5.7). As our main emphasis is robust and accurate stress approximation, we briefly discuss some choices toward the achievement of this aim. We denote the space of continuous piecewise polynomials of degree (less than or equal to) k defined relative to a simplicial tessellation $\mathcal{T}_h$ by $\mathcal{P}_k^c(\mathcal{T}_h)$, and the space of discontinuous piecewise polynomials by $\mathcal{P}_k(\mathcal{T}_h)$. The space of piecewise polynomial vector fields of degree k with continuous normal components over edges (or faces) is labeled $\mathrm{BDM}_k(\mathcal{T}_h)$ (cf. [6, 22]), with $\mathrm{BDM}_k(\mathcal{T}_h; \mathbb{V}) = \mathrm{BDM}_k(\mathcal{T}_h)^n$.

First, for discretizations $U_h \times P_h \subset H^1(\Omega; \mathbb{V}) \times L^2(\Omega)$ of the displacement-pressure formulation (5.1), we use the generalized Taylor–Hood elements: for $k = 1, 2, \ldots$, continuous piecewise $(k+1)$th degree polynomial fields for the displacement, and continuous piecewise kth degree fields for the pressure. The lowest order elements are thus

$$U_h \times P_h = \mathcal{P}_2^c(\mathcal{T}_h; \mathbb{V}) \times \mathcal{P}_1(\mathcal{T}_h). \tag{5.16}$$

For smooth solutions, $(k+1)$th order convergence is expected in the H^1-norm of the displacement and hence for a postcalculated stress tensor as well.

Second, for the nearly symmetric stress-displacement-rotation formulation (5.7), we utilize the lowest order element spaces of the family suggested by Farhloul and Fortin [13] and Falk [12]; specifically, for $k = 1, 2, \ldots$, piecewise kth degree polynomial tensor fields with row-wise normal component continuity for the stresses, discontinuous $(k-1)$th degree for the displacements, and continuous kth degree for the rotations. The lowest order is

$$\Sigma_h \times V_h \times Q_h = \mathrm{BDM}_1(\mathcal{T}_h; \mathbb{V}) \times \mathcal{P}_0(\mathcal{T}_h; \mathbb{V}) \times \mathcal{P}_1^c(\mathcal{T}_h; \mathbb{K}). \tag{5.17}$$

For our purposes, these elements are preferable to the similar spaces considered by Arnold, Falk, and Winther [2] because the higher order stress interpolation error is conserved at little additional cost. As for the displacement-pressure discretization, the discretization defined by (5.17) gives $(k+1)$th order convergence for the stress tensor for smooth solutions.

Thus, in theory, both formulations with the previously described discretizations give the same order of convergence for the stresses. One advantage of the displacement-pressure approach is that it is typically less expensive than the stress-displacement-rotation approach. This aspect may be particularly relevant in three dimensions. However, the disadvantage to using this method is that the stress tensor must be postcalculated. This is evidently not an issue with the stress-displacement-rotation approach. An additional advantage of the stress-displacement-rotation approach is that it gives stress tensors with normal component continuity and hence

continuous stresses over interelement boundaries. The latter consequence is particularly relevant if there are internal interfaces in the domain where the interfacial stress is a quantity of interest.

6. Simulations. In this section, we present some numerical simulations. First, we examine the stability range of the nearly symmetric stress-displacement-rotation formulation numerically in order to compare the observations with the analytical estimates. Next, we turn to a more physically realistic application. The gel model and numerical methods presented are applied to studying the shear stresses arising from the confinement and environmental effects experienced by an artificial bone implant. All simulations have been performed using the DOLFIN library of the FEniCS project [14, 20].

6.1. Numerical stability of nearly symmetric stress formulation. The residual stress r clearly has an impact on the approximation properties of discretizations of the nearly symmetric stress formulation. In order to numerically investigate this effect, we consider a range of values for r and compare the error of approximation and the rate of convergence for a given discretization of (5.7). We remark that such a study can be performed independently of the specific expressions for the Lamé parameters given by (4.9). However, using a range of values for μ and λ relevant for the gel model seems appropriate. In lieu of (4.9) and (5.12), we let $\mu = 1.0$, consider a set of positive λ, and let $r \in (-1.5\,\mu, 2\mu)$.

The following domain and exact smooth solutions are considered in order to examine the error and the convergence rate of the approximations. We let $\Omega = (0,1)^2 \subset \mathbb{R}^2$ and consider the boundary $\partial\Omega = \partial\Omega_0 \cup \partial\Omega_1$, where

$$\partial\Omega_0 = \{X \in \partial\Omega,\, X_0 \in \{0,1\}\}, \quad \partial\Omega_1 = \partial\Omega \backslash \partial\Omega_0.$$

Define the following smooth displacement:

$$u = u(x_0, x_1) = (\sin(\pi x_0), \sin(\pi x_0)). \tag{6.1}$$

For a given r, we define the associated stress tensor σ^r and rotation γ^r in accordance with (4.8) and (5.4), respectively. We also let $g^r = \operatorname{div} \sigma^r$ and $s_0^r = \sigma^r \cdot n$ on $\partial\Omega_1$. By construction, σ^r, u, and γ solve (5.7) with the boundary conditions $u|_{\partial\Omega_0} = 0$ and $\sigma^r \cdot n|_{\partial\Omega_1} = s_0^r$. Furthermore, we let $\mathcal{T}_h$ be a uniform, regular triangulation of Ω, and we consider the discretization defined by (5.17). Recall that if the residual stress r, viewed in connection with the Lamé coefficients μ and λ, is such that (5.12) holds, we expect second order convergence for the stress approximations in the L^2-norm.

The relative error of the stress approximation for a given meshsize $h = 1.0/40$ and the rate of convergence for the stress in the L^2-norm between $h = 1.0/20$ and $h/2 = 1.0/40$ are plotted in Figure 6.1 for $\lambda \in \{1.0, 10.0, 100.0\}$. We observe that, for $\lambda = 1.0$, the relative error of the approximation seems uniform for $-0.5 < r < 1.0$, and the convergence rate is of second order. For $r < -0.5$, the relative error grows in a nonregular fashion, and the convergence rates vary dramatically. Further investigations show that the convergence rates are also highly dependent on the meshsize. The observed behavior agrees with the theoretical results. The method is not guaranteed to be stable for r sufficiently negative. Indeed, the above observations give evidence of instabilities for $r < -0.5$. We note that no instability is observed for r close to 1.0, indicating that the requirement $r > \mu$, motivated by $k_r > 0$, could be relaxed. For $r \to 2.0$, we note only a slight increase in the relative error and no observed variation in the convergence rate. This indicates that the stress approximation is only slightly

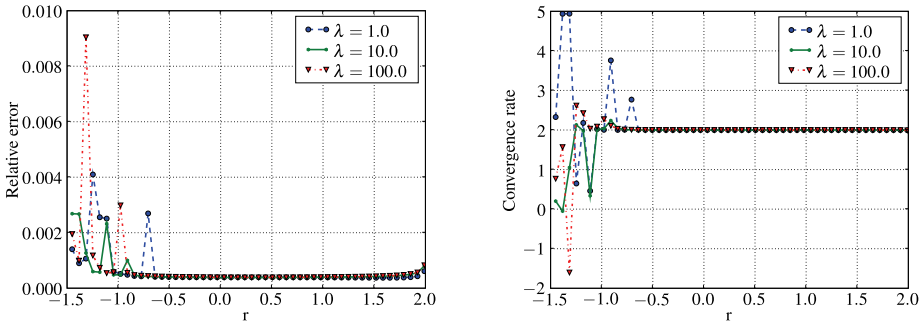

FIG. 6.1. *Approximation properties of the nearly symmetric formulation in terms of the residual stress for* $\lambda = 1, 10, 100$. *Left: Stress approximation errors. Relative error* E_r *of the stress approximation versus residual stress* r. $E_r = ||\sigma^r - \sigma_h^r||_0/||\sigma^r||_0$. $h = 1.0/40$. *Right: Convergence rates. Convergence rate* c_r *of the stress approximations versus residual stress* r. $c_r = ||\sigma_{h/2}^r||_0/||\sigma_h^r||$. $h = 1.0/20$.

affected by the small coercivity constant. The cases $\lambda = 10.0$ and $\lambda = 100.0$ are entirely analogous to the case $\lambda = 1.0$. This indicates that increasing λ does not have a deleterious impact on the performance of the method.

6.2. Swelling-induced stress in artificial bone implants. We now turn to consider a specific biomedical application: an artificial bone implant used for high tibial osteotomy. In this procedure, the knee is realigned to shift the body weight from a damaged area of the knee to the side with healthy cartilage. This is performed by removing a wedge from the shinbone and then chemically gluing a polymer implant into the open space in order to realign the knee. One natural question that arises is whether and how the additional moisture of the body affects the implant. Another relevant question is how the confinement of the gel affects the stresses. In particular, both the implant itself and the glue attaching the implant to the bone may fail when exposed to high shear forces.

In the following, we aim to apply the appropriately linearized gel equations and the numerical methods of the previous sections to examine the shear stresses acting on the implant. First, we study the stresses arising from the confinement of an implanted polymer gel. Second, using the approximation given in (4.4), we investigate how temperature changes in the body may affect the implant. Finally, an interface problem between the bone and the implant is considered. Although we consider a specific device, the simulations illustrate the more general situation of swelling in a confined area under environmental and mechanical forces.

Polymers used in biomedical devices which provide mechanical reinforcement must have low interaction with water and be rigid so as to prohibit large swelling. The following homogeneous parameter values are representative of polymers used in artificial bone implants [33, 21]. In (2.8) and (2.6), we let $V_m = 0.1\text{nm}^3$, $N_1 = 1000$, $N_2 = 1$, $\mu_E = 1.0$ GPa, $\beta = 2$, $\Delta w = (150\,\text{K})K_B$, and consider an initial temperature $T = 310$ K. The choice of Δw is such that $\chi(T) = 0.5$ at $T = 300$ K, in agreement with [33]. The associated Flory–Huggins energy density has a single minimum at $\phi_I^N \approx 0.66$ and hence $r(\phi_I^N) = 0$. A physically realistic value for the volume fraction of the polymer, however, is typically close to 1. With this in mind, we consider a set of reference volume fraction values ϕ_I in the range $[0.6, 1.0)$.

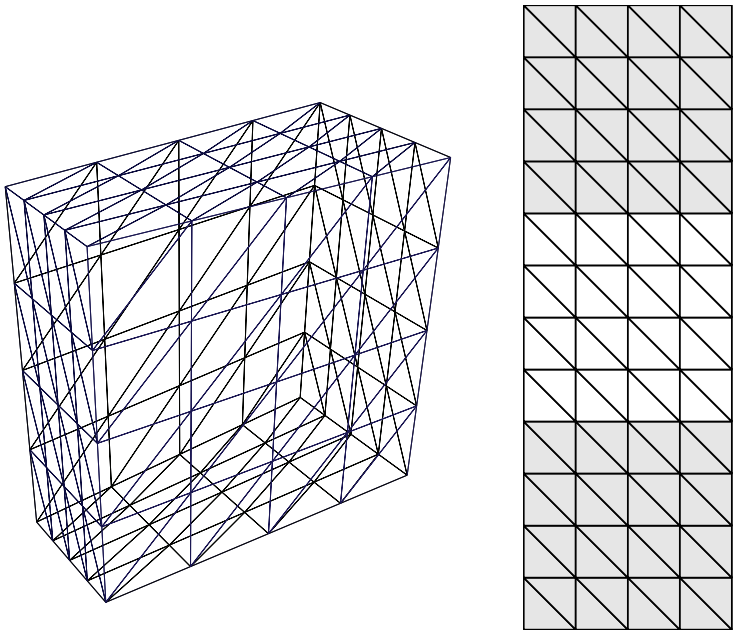

(a) (b)

FIG. 6.2. *The simulation domains.* (a) *An illustration of the three-dimensional wedge domain* Ω *occupied by the gel in the artificial bone implant simulation. Shown here is a coarse tessellation of the domain from a top, left view.* (b) *A coarse triangulation of the cross-sectional domain occupied by the gel and the bone.*

Confinement. If the reference volume fraction is higher than the volume fraction corresponding to a stress-free reference state, the gel will respond with an initial swelling. In order to isolate this effect, we consider the linearized equations about a nonidentity state $F_0 = f_0 I$ such that $\mathcal{S}(F_0) = 0$; cf. (4.10). For $\phi_I = 0.995$, $f_0 \approx 1.0038$. The equations to be considered are thus those of Problem 1 with $f, g = 0$ but with μ and λ given by (4.11). The nonidentity linearization has ramifications for the boundary conditions. Since the total deformation can be given as $x(X) = u(X) + f_0 X$, in order to represent a bone implant entirely confined at some $\partial\Omega_0$, we let

$$u(X) = u_0(X) = (1 - f_0)X, \quad X \in \partial\Omega_0, \tag{6.2}$$

thus ensuring no deformation of the reference body at the given boundary. However, for $f_0 \neq 1$, the inclination to swell versus the confinement of the implant yields a nonzero u_0. In particular, shear stress forces are induced. At $\partial\Omega_1$, we let $\sigma \cdot n = s_0 = 0$.

Motivated by typical implant shapes, we consider a hexahedral reference domain for the bone implant defined by an isosceles trapezoidal base. More precisely, let $\Omega^0 = (0, 20) \times (0, 10) \times (0, 20)$ (mm^3) and, in general, $\Omega^\theta = \{(X_0, X_1, X_2)\} \subseteq \Omega^0$ such that

$$X_1 \in ((2 - X_0)\tan(\theta), 1 - (2 - X_0)\tan(\theta))$$

for $0 \leq \theta \leq \theta_{\max} = \arctan(1/4)$. Thus, $\Omega^{\theta_{\max}}$ is defined by an isosceles triangular base. In the following, we consider $\theta = \arctan(1/16)$. This domain is illustrated in Figure 6.2(a). Further, the implant is assumed to be confined at the top and bottom

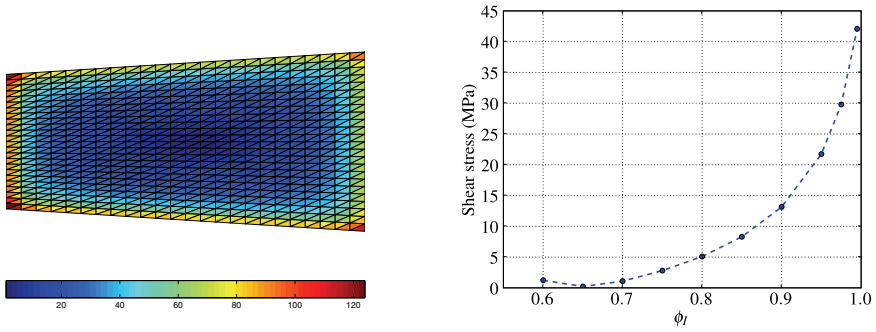

(a) (b)

FIG. 6.3. *Shear stresses, in MPa, resulting from the confinement of a gel in a nonequilibrium state.* (a) *The magnitude of the shear stress vector measured at the barycenters of each facet of the top boundary* Γ *for* $\phi_I = 0.995$. (b) *The average shear stress over the top boundary* S_Γ *versus initial volume fraction* ϕ_I.

boundaries, where it adjoins the bone, and stress-free at the remaining boundary:

$$\partial\Omega_0 = \{X \in \partial\Omega,\, X_2 \in \{0, 2\}\}, \quad \partial\Omega_1 = \partial\Omega \backslash \partial\Omega_0. \tag{6.3}$$

The resulting boundary value problem was simulated using the displacement-pressure formulation (5.1) with the Taylor–Hood elements (5.16) on a regular tessellation of Ω consisting of approximately 80,000 tetrahedral cells. The stress tensor was postcalculated from the displacement and the pressure approximations using (4.7a). The quantity of interest is the shear stress at the top and bottom boundaries of the implant. Due to symmetry, we consider only the top boundary Γ. The magnitude of the tangential component of the stress at the barycenter of each facet at the top boundary is shown in Figure 6.3(a) for $\phi_I = 0.995$. The reported values are in the range $(0, 125)$ MPa but should be interpreted qualitatively. We see that the stresses are, relatively speaking, low in the interior of the top boundary, but that a boundary layer forms, which gives very high stress values at the corners. In fact, these pointwise stress values do not seem to be bounded, in the sense that the maximal value depends on the meshsize. Considering the unreliability of this pointwise stress magnitude, we instead measure the average shear stresses over the top boundary:

$$S_\Gamma^2 = \frac{1}{\int_\Gamma 1 \,\mathrm{ds}} \left(\int_\Gamma \sigma_{02}^2 + \sigma_{12}^2 \,\mathrm{ds} \right). \tag{6.4}$$

The shear stresses S_Γ corresponding to ϕ_I in the range $[0.60, 1.0)$ are plotted in Figure 6.3(b). We see that the average shear stress is close to zero for $\phi_I = 0.65$, as this is close to the natural volume fraction of the energy. The average shear stresses grow as ϕ_I approaches 1.0: at $\phi_I = 0.995$, the average shear stress is approximately 42.1 MPa. We conclude that the confinement versus the swelling gives significant shear stress values for the implant.

Temperature. We now turn to inspecting how an increase in temperature affects the implant. In order to obtain a qualitative understanding of the effects of changes in temperature, we consider a perturbation about the initial temperature, as discussed in connection with (4.4). The temperature dependence of the given model occurs only through the coefficients of the Flory–Huggins potential, and thus (cf. (4.2)) the

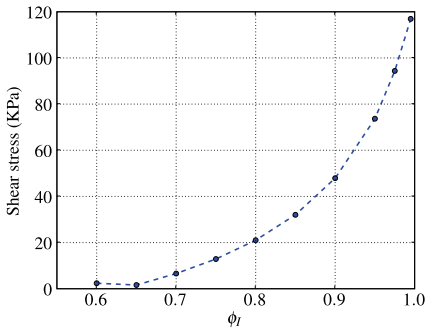

FIG. 6.4. *Shear stresses, in KPa, resulting from temperature changes. Average shear stress over the top boundary S_Γ versus initial volume fraction ϕ_I.*

resulting force f reads

$$f = f(\Delta T) = \frac{\partial}{\partial T}\left(\mathcal{W}_{FH}(\phi, T) + c_{FH}(T) - \phi \mathcal{W}'_{FH}(\phi, T)\right)(\Delta T)\,(\det F)F^{-T}.$$

We let $T = 310$ K as before and consider $\Delta T = 1.0$. The parameter values, domain, and discretization are as for the previous experiment. The resulting pressure force is of the order 0.4 MPa for $\phi_I = 0.995$ and thus two orders of magnitude smaller than the shear stresses resulting from the confinement. In order to isolate the effects of the change in temperature, we modify the boundary conditions of (6.2) and let $u_0 = 0$ on $\partial\Omega_0$. This corresponds to letting the implant swell to the equilibrium position and penalizing the additional swelling resulting from the changes in temperature only.

The resulting average shear stresses at the top boundary of the implant, following the same procedure as in the previous, are illustrated in Figure 6.4. Note the difference in units between Figures 6.3(b) and 6.4. The average shear stress values are in the range $(1.61, 117)$ KPa and thus significantly lower than those associated with the full confinement.

Gel-bone interaction. Finally, we consider the interface problem between the gel implant and the bone to which it is attached. In the first experiment of this section, the implant was assumed to be entirely confined at the top and bottom boundary. This assumption does not take the elastic properties and behavior of the bone into account. In particular, in reality, it seems meaningful to assume that the bone will absorb some of the swelling of the gel. Here, we examine the shear stresses of the gel-bone interface when the bone is assumed to be linearly elastic. In particular, we consider a two-dimensional cross section, in the longitudinal direction, of the gel implant and the bone.

Let $\Omega = (0, 20) \times (0, 60)\,\text{mm}^2$. This reference domain is illustrated in Figure 6.2(b). The lower and upper interfaces between the gel and the bone are placed at the line segments defined by $X_1 = 20.0$ and $X_1 = 40.0$, respectively. Thus, the middle third of the domain is occupied by the gel, while the upper and lower thirds are occupied by the bone. We assume that the bone is confined at the top and bottom boundaries, that is, at the line segments defined by $X_1 = 0$ and $X_1 = 60$. Both the bone and the gel are assumed to be stress-free at the left and right boundaries.

The gel parameter values and the range of reference volume fractions to be considered are as before. However, instead of linearizing about a nonidentity but stress-free

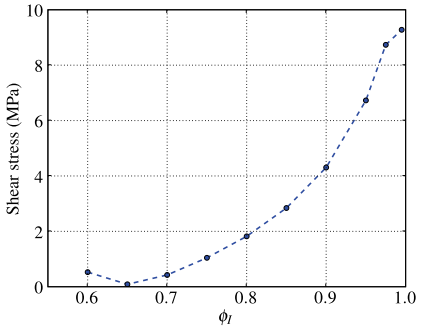

FIG. 6.5. *Average shear stress, in MPa, over the upper gel-bone boundary* $S_{\Gamma_{\mathrm{gb}}}$ *versus initial volume fraction* ϕ_I.

state, we now consider the small-strain equations resulting from the linearization about the identity deformation. Thus, the Lamé parameters of the gel, $\mu(\phi_I)$ and $\lambda(\phi_I)$, are as defined by (4.9). The residual stress $r(\phi_I)$ will act as a forcing term; cf. (4.7a). We remark that for the above parameter values and the given range of reference volume fractions, $r(\phi_I) \in (-0.17, 0.0036)$. Furthermore, we give the bone the Lamé parameters $\mu_{\mathrm{b}} = 4.0$ GPa and $\lambda_{\mathrm{b}} = 20.0$ GPa. Under these assumptions, both the bone and the gel are governed by (4.7). The Lamé parameters μ and λ, however, are now heterogeneous.

As in the previous, any nonequilibrium gel reference volume fraction ϕ_I will produce a swelling or collapse of the domain. Our main interest lies with the shear stresses at the upper and lower material interfaces. As these are interfaces in the interior of the domain, the stress-displacement-rotation formulation (5.7) and the discretization defined by (5.17) are used for this simulation. We denote the upper gel-bone interface by Γ_{gb}. Keeping with the previous, we consider the average shear stress over this interface:

$$S^2_{\Gamma_{\mathrm{gb}}} = \frac{1}{\int_{\Gamma_{\mathrm{gb}}} 1 \,\mathrm{ds}} \left(\int_{\Gamma_{\mathrm{gb}}} \sigma^2_{01} \,\mathrm{ds} \right).$$

The triangulation used for the simulation contains approximately 25,000 triangles. The simulated average shear stress values are plotted versus the reference volume fraction in Figure 6.5. For $\phi_I = 0.65$, $S_{\Gamma_{\mathrm{gb}}} \approx 8.81 \times 10^{-2}$ MPa. This relatively small value is expected, as this volume fraction is close to the reference volume fraction with zero residual stress. The shear stresses increase as the volume fraction increases: at $\phi_I = 0.995$, $S_{\Gamma_{\mathrm{gb}}} \approx 9.28$ MPa. We note that the shear stresses are smaller than those resulting from the total confinement, but still significant.

7. Conclusion. We have presented a study of gel equilibrium problems designed to model the behavior of a polymeric biomedical device upon implantation into the human body. One motivation for studying such problems is to facilitate effective device design. Upon implantation, the moisture of the body causes the device to swell. That, combined with the confinement of the device, induces stress concentrations near the attachments. In particular, the shear components of the stress may cause the detachment and failure of the device. Thus, both understanding the source of stresses and predicting the magnitudes of such stresses are important for successful device design.

The equilibrium equations considered combined an elastic energy and a mixing energy derived from Flory–Huggins theory. Two numerical methods were proposed and analyzed for the small-strain equations: a two-field displacement-pressure formulation and a three-field stress-displacement-rotation formulation. The simulations presented focused on the computation of shear stresses resulting from residual stress in combination with confinement and from temperature fluctuations. All simulations were implemented using the free FEniCS software, which provides a flexible and mathematically well-developed finite element framework. We note that this software could potentially serve the scientific community as a useful tool for studying gels.

The results showed that the stresses due to the combination of residual stress and confinement are much more pronounced than those due to temperature fluctuations; indeed, the temperature effects are only a small perturbation of the confinement effects. These results suggest that the confinement of a swelling gel is the dominant source of stress in such devices. We remark that the equilibrium framework studied provides only an approximation to the more physically realistic time evolution undergone by gels. However, the results obtained support the idea that equilibrium analysis is a good approximate method of stress prediction.

Acknowledgments. The authors wish to thank Suping Lyu, Medtronic, Inc., for supplying appropriate material parameters. The first author also wishes to thank Ragnar Winther for fruitful discussions and comments on the manuscript.

REFERENCES

[1] E. S. Almeida and R. L. Spilker, *Mixed and penalty finite element models for the nonlinear behaviour of biphasic soft tissues in finite deformation: Part* I*—Alternate formulations*, Comput. Methods Biomech. Biomed. Engrg., 1 (1997), pp. 25–46.

[2] D. N. Arnold, R. Falk, and R. Winther, *Mixed finite element methods for linear elasticity with weakly imposed symmetry*, Math. Comput., 76 (2007), pp. 1699–1723.

[3] D. N. Arnold and R. Winther, *Mixed finite elements for elasticity*, Numer. Math., 92 (2002), pp. 401–419.

[4] J. M. Ball, *Convexity conditions and existence theorems in nonlinear elasticity*, Arch. Ration. Mech. Anal., 63 (1977), pp. 337–403.

[5] D. Braess, *Finite Elements: Theory, Fast Solvers, and Applications in Solid Mechanics*, Cambridge University Press, Cambridge, UK, 2001.

[6] F. Brezzi, J. Douglas, Jr., and L. D. Marini, *Two families of mixed finite elements for second order elliptic problems*, Numer. Math., 47 (1985), pp. 217–235.

[7] F. Brezzi and M. Fortin, *Mixed and Hybrid Finite Element Methods*, Springer–Verlag, New York, Berlin, 1991.

[8] M. C. Calderer, B. Chabaud, S. Lyu, and H. Zhang, *Modeling approaches to the dynamics of hydrogel swelling*, J. Comput. Theoret. Nanosci., (2008), to appear.

[9] P. G. Ciarlet, *Mathematical Elasticity, Volume* I: *Three-Dimensional Elasticity*, North–Holland, Amsterdam, 1988.

[10] J. Dolbow, E. Fried, and H. Ji, *Chemically induced swelling of hydrogels*, J. Mech. Phys. Solids, 52 (2004), pp. 51–84.

[11] J. Dolbow, E. Fried, and H. Ji, *A numerical strategy for investigating the kinetic response of stimulus-responsive hydrogels*, Comput. Methods Appl. Mech. Engrg., 194 (2005), pp. 4447–4480.

[12] R. S. Falk, *Finite element methods for linear elasticity*, in Mixed Finite Elements, Compatibility Conditions and Applications, D. Boffi and L. Gastaldi, eds., Lecture Notes in Math. 1939, Springer-Verlag, New York, 2008, pp. 160–194.

[13] M. Farhloul and M. Fortin, *Dual hybrid methods for the elasticity and the Stokes problem: A unified approach*, Numer. Math., 76 (1997), pp. 419–440.

[14] The FEniCS Project, *FEniCS*, software for solution of differential equations, online at http://www.fenics.org/.

[15] P. J. Flory, *Principles of Polymer Chemistry*, Cornell University Press, Ithaca, NY, 1953.

[16] D. R. Gaskell, *Introduction to the Thermodynamics of Materials*, Taylor & Francis, Oxford, UK, 1995.
[17] W. Hong, Z. Liu, and Z. Sou, *Inhomogenous swelling of a gel in equilibrium with a solvent and mechanical load*, Internat. J. Solids Structures, 46 (2009), pp. 3282–3289.
[18] W. Hong, X. H. Zhao, J. X. Zhou, and Z. G. Suo, *A theory of coupled diffusion and large deformation in polymeric gels*, J. Mech. Phys. Solids, 56 (2008), pp. 1779–1793.
[19] M. Kleman and O. Lavrentovich, *Soft Matter Physics: An Introduction*, Springer–Verlag, New York, Berlin, 2003.
[20] A. Logg and G. N. Wells, *DOLFIN: Automated finite element computing*, (2009), submitted.
[21] S. Lyu, *personal communication*, data provided by Medtronic, Inc.
[22] J. C. Nédélec, *A new family of mixed finite elements in* $\mathbf{R}^3$, Numer. Math., 50 (1986), pp. 57–81.
[23] Y. Osada and K. Kajiwara, eds., *Gels Handbook*, Academic Press, New York, 2001.
[24] M. Rubinstein and R. Colby, *Polymer Physics*, Oxford University Press, Oxford, UK, 2003.
[25] D. J. Segalman and W. R. Witkowski, *Two-dimensional finite element analysis of a polymer gel drug delivery system*, Mater. Sci. Engrg. C, 2 (1995), pp. 243–249.
[26] H. C. Simpson and S. J. Spector, *On copositive matrices and strong ellipticity for isotropic elastic materials*, Arch. Ration. Mech. Anal., 84 (1983), pp. 55–68.
[27] T. Tanaka, *Collapse of gels and the critical endpoint*, Phys. Rev. Lett., 40 (1978), pp. 820–823.
[28] C. Truesdell, *Rational Thermodynamics*, Springer–Verlag, New York, Berlin, 1984.
[29] T. Yamaue and M. Doi, *Swelling dynamics of constrained thin-plate gels under an external force*, Phys. Rev. E, 70 (2004), paper 011401.
[30] T. Yamaue and M. Doi, *Theory of one-dimensional swelling dynamics of polymer gels under mechanical constraint*, Phys. Rev. E, 69 (2004), paper 041402.
[31] T. Yamaue and M. Doi, *The stress diffusion coupling in the swelling dynamics of cylindrical gels*, J. Chem. Phys., 122 (2005), paper 084703.
[32] H. Zhang, *Static and Dynamical Problems of Hydrogel Swelling: Modeling and Analysis*, Ph.D. thesis, School of Mathematics, University of Minnesota, Twin Cities, MN, 2007.
[33] H. Zhang and M. C. Calderer, *Incipient dynamics of swelling of gels*, SIAM J. Appl. Math., 68 (2008), pp. 1641–1664.